Rotational Dynamics of the Single Tryptophan of Porcine Pancreatic Phospholipase A_2, Its Zymogen, and an Enzyme/Micelle Complex. A Steady-State and Time-Resolved Anisotropy Study†

Richard D. Ludescher,[‡,§,∥] Iain D. Johnson,[‡] Johannes J. Volwerk,[§] Gerard H. de Haas,[⊥] Patricia C. Jost,[§,#] and Bruce S. Hudson*[,‡,§]

Department of Chemistry and Institute of Molecular Biology, University of Oregon, Eugene, Oregon 97403, and State University of Utrecht, Utrecht, The Netherlands

Received November 10, 1987

ABSTRACT: The rotational dynamics of the single tryptophan of porcine pancreatic phospholipase A_2 and its zymogen (prophospholipase A_2) have been studied by polarized fluorescence using steady-state and time-resolved single-photon counting techniques. The motion of Trp-3 in phospholipase A_2 consists of a rapid subnanosecond wobble of the indole ring with an amplitude of about ±20° accompanied by slower isotropic rotation of the entire protein. The rotational correlation times for overall particle rotational diffusion are consistent with conventional hydrodynamic theory. When phospholipase A_2 binds to micelles of *n*-hexadecylphosphocholine, the amplitude of the fast ring rotation decreases. The whole particle rotational correlation time of the enzyme/micelle complex is smaller than the minimum value calculated from hydrodynamic theory. A similar result is obtained for the micelle itself by using the lipophilic probe *trans*-parinaric acid. These low values for the particle correlation times can be understood by postulating that an isotropic motion of the fluorophore in the small detergent particles contributes to the angular reorientation of the fluorophore. The internal reorientational motion of the tryptophan in the zymogen, prophospholipase A_2, is of larger amplitude than that observed for the enzyme; specifically, the proenzyme exhibits a motion with a significant amplitude on the nanosecond time scale. This additional freedom of motion is attributed to segmental mobility of the N-terminal residues of prophospholipase A_2. This demonstrates that this region of the protein is flexible in the zymogen but not in the processed enzyme. The implications of these findings for the mechanism of surface activation of phospholipase A_2 are discussed by analogy with a trypsinogen–trypsin activation model.

Porcine pancreatic phospholipase A_2 (phosphatide acylhydrolase EC 3.1.1.4; PLA_2[1]) is a 13 800-dalton enzyme that is synthesized as a zymogen, $ProPLA_2$, with an extra seven amino acids at the N-terminus. Both the zymogen and the enzyme can hydrolyze the 2-acyl ester bond of monomeric 3-*sn*-phosphoglycerides. Only PLA_2, however, can hydrolyze lipids organized into aggregates (micelles or monolayers) [see Volwerk and de Haas (1982) for a review]. Semisynthetic studies of PLA_2 (Slotboom et al., 1978; Jansen, 1979) have demonstrated that the hydrophobic moiety of the tryptophan residue at position 3 (Trp-3), the only tryptophan in the protein, is essential for PLA_2 binding to lipid–water interfaces. The pronounced perturbations of the absorption and fluorescence spectra of Trp-3 in PLA_2 that occur in the presence of micellar aggregates of nonhydrolyzable substrate analogues are consistent with the transfer of Trp-3 from an aqueous to a hydrophobic environment and support the notion that the tryptophan plays a central role in binding to lipid aggregates (Van Dam-Mieras et al., 1975; Ludescher et al., 1985).

A schematic representation of the structure of bovine PLA_2 as determined by Dijkstra et al. (1978) is illustrated in Figure 1. This structure has been refined to 1.7-Å resolution (Dijkstra et al., 1981a) and is essentially identical with that of the porcine enzyme used in the present study (Dijkstra et al., 1983). The only major difference between the two structures is in the region of residues 59–70. The α-helix (helix D) in this region of the bovine enzyme is replaced in the porcine enzyme by a short stretch of 3/10 helix (Dijkstra et al., 1983). Both the bovine and the porcine enzymes contain about 50% α-helix and 10% β-sheet structure and have seven disulfide bonds. The active site of the enzyme is located in the cleft between helices A, B, and C and the random coil to the C-terminal side of helix B. The lone tryptophan, located at position 3, is on the side of helix A that faces away from the active site. The tryptophan ring is flat against the protein surface in a shallow cleft between helix A and one strand of the two-strand β-sheet that forms one entire side of the protein. In the bovine structure, the indole ring lies directly over the amide function of Gln-4. The indole N–H is involved in a bifurcated hydrogen bond to a water residue and Asn-72. Although the lower resolution of the porcine structure does

† This study is, in part, abstracted from the Ph.D. dissertation of R.D.L., who was an NIH predoctoral trainee (GM07759) during the course of this research. The support of the National Institute of Health (Grants GM26536 and GM25698) is gratefully acknowledged. A preliminary report of this research was presented at the 27th Annual Meeting of the Biophysical Society, Feb 13–16, 1983.

* Address correspondence to this author at the Department of Chemistry.

‡ Department of Chemistry.

§ Institute of Molecular Biology.

∥ Present address: Department of Chemistry, The Wichita State University, Wichita, KS 67208.

⊥ State University of Utrecht.

Present address: Division of Research Grants, National Institutes of Health, Bethesda, MD 20892.

[1] Abbreviations: $C_{16}PN$, *n*-hexadecylphosphocholine; LSIR, least-squares iterative reconvolution; MCP, microchannel plate detector; PLA_2, porcine pancreatic phospholipase A_2; PMT, photomultiplier; $ProPLA_2$, porcine pancreatic prophospholipase A_2.

0006-2960/88/0427-6618$01.50/0

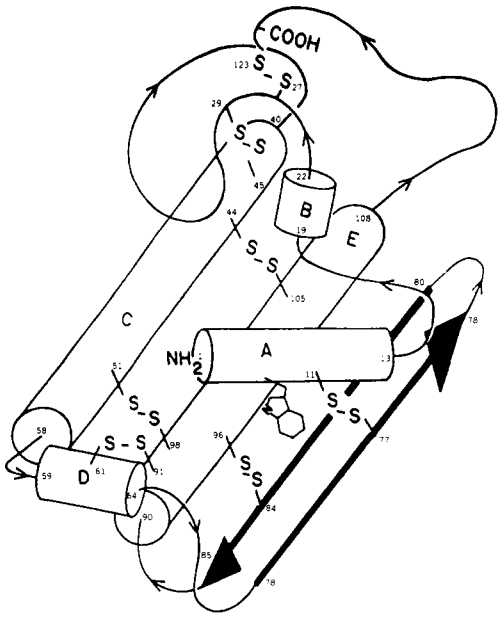

FIGURE 1: Secondary structure and folding pattern of bovine phospholipase A_2 taken from Dijkstra et al. (1978). The single tryptophan in the molecule is indicated. The recently reported structure of porcine PLA_2 (Dijkstra et al., 1983) is nearly identical with this structure.

not allow such a detailed description of the tryptophan environment, it appears that the N-terminal structures of the two proteins are nearly identical.

The crystal structure of the bovine zymogen $ProPLA_2$ has been determined to 3.0-Å resolution by Dijkstra et al. (1982) and is nearly identical with that of the processed enzyme. The major differences occur in the residues of the loop from 62 to 74, which are more disordered in the zymogen, and in the N-terminal region (including Trp-3),[2] which is not visible in the electron density map of $ProPLA_2$. There is currently no reliable crystal structure of porcine $ProPLA_2$.

These proteins offer an excellent system for a fluorescence study of the relationship between structure and tryptophan dynamics for a functionally important Trp residue (Hudson et al., 1986, 1987). There is only one tryptophan in these proteins, and it plays a central role in the binding of PLA_2 to lipid aggregates. The steady-state and time-resolved anisotropy measurements reported here indicate that Trp-3 has a different range of motion in $ProPLA_2$ and PLA_2 and in the complex of PLA_2 with the nonhydrolyzable substrate analogue *n*-hexadecylphosphocholine. These dynamic measurements are an extension of a study of the decay of the total fluorescence intensity of Trp-3 in these proteins (Ludescher et al., 1985), where it was shown that the decay of the fluorescence is very complex.

Materials and Methods

Sample Preparation. The zymogen of phospholipase A_2 was isolated from hog pancreas and converted into fully active enzyme by limited proteolysis as described in Nieuwenhuizen et al. (1974). $C_{16}PN$ was synthesized as described in Van Dam-Mieras et al. (1975). All protein and lipid solutions were prepared in 0.1 M sodium acetate buffer, pH 6.0, by using glass-distilled water. Protein was stored as lyophilized powder at −20 °C and dissolved in buffer prior to use at concentrations near 10 μM. The complex of PLA_2 with $C_{16}PN$ detergent was prepared at a detergent/protein ratio of 500 with a final detergent concentration of 5 mM. The concentration of protein was determined from the optical density at 280 nm using $E^{1\%}$ of 13.0 for PLA_2 and 12.3 for $ProPLA_2$ (Van Dam-Mieras et al., 1975). The trans isomer of parinaric acid was obtained from Molecular Probes, Inc. (Eugene, OR) and stored in ethanol as a 3 mM solution at −20 °C. The micelles were labeled by addition of an aliquot of the ethanol solution directly to the sample cuvette. The final ethanol concentration was always less than 0.1%, and the optical density at the excitation wavelength was kept below 0.05.

Steady-State Anisotropy. Steady-state anisotropy ($\langle r \rangle$) measurements were made with an SLM-8000 spectrofluorometer (SLM Industries, Urbana, IL) using 300-nm excitation (4-nm slits) and 350-nm emission (8-nm slits). The temperature was controlled with a water bath connected to a jacketed cuvette holder. The optical density at the excitation frequency was always less than 0.05 for all anisotropy measurements (including time-resolved). The ratio $R = (I_{vv}/I_{hv})/(I_{vh}/I_{hh})$, where I_{ij} represents intensity collected with excitation polarization i and emission polarization j, was measured and used to calculate $\langle r \rangle = (R - 1)/(R + 2)$. Steady-state fluorescence anisotropy measurements were also made as a function of excitation wavelength by using a 2-nm bandpass for excitation with 350-nm emission with a 16-nm bandwidth.

Solution viscosity was varied by changing temperature or by addition of glycerol (Aldrich Gold Shield). Values for the water viscosity as a function of temperature or weight percent glycerol were taken from the *CRC Handbook of Chemistry and Physics, 59th Edition.*

Steady-state anisotropy measurements were analyzed in a manner similar to that described by Lakowicz et al. (1983) and Eftink (1983). The steady-state anisotropy was measured as a function of solution viscosity by varying temperature. A plot of $1/\langle r \rangle$ vs T/η was generated and extrapolated to $T/\eta = 0$. The reciprocal of the y intercept is an effective r_0, $(r_0)_{eff}$. The difference between this value and the true r_0 for the fluorophore is a measure of the amplitude of any rapid internal motions of the fluorophore in the protein.

Time-Resolved Anisotropy Measurements. Time-resolved anisotropy measurements were performed by using a high-repetition rate synchronously pumped dye laser with single-photon counting detection procedures. In one configuration, a mode-locked argon ion laser was used as the excitation source; an RCA 31000M photomultiplier (PMT) was used as the single-photon counting detector. In this case the instrumentation is the same as that described in Ludescher et al. (1985) and Small et al. (1984). The instrument resolution function for this PMT apparatus was about 700 ps. Some of the experiments have been repeated with a microchannel plate (MCP) based system that uses a mode-locked, frequency-doubled Nd:YAG laser as the excitation source for the dye laser. This device is described in detail elsewhere (Ruggiero & Hudson, 1987). The instrument response of this MCP system is ca. 90 ps. Anisotropy decays were measured by using vertically polarized excitation by collecting a lamp profile (i.e., the machine response function) as light scattered from a ludox sample and collecting a fluorescence decay from the sample alternating between vertically and horizontally polarized emission. Collection time was 60 s, and the cycle was repeated usually 15–20 times under the control of a microcomputer. A typical experiment had greater than 5×10^6 total counts in the difference decay with a peak in excess of 10^5 counts. The fluorometer has only a small polarization bias, so a "*G* value" (equal to I_{hv}/I_{hh}) within 5% of unity was used in all

[2] The residues of the zymogen are numbered from −7 in order to maintain correspondence with the active enzyme form.

analyses. The anisotropy decays were composed channel by channel according to the defining equation (for $G = 1$)

$$r(t) = [I_{vv}(t) - I_{vh}(t)]/[I_{vv}(t) + 2I_{vh}(t)] = D(t)/I(t) \quad (1)$$

Time-Resolved Anisotropy Analysis. Decay parameters were extracted from the experimental decays by using least-squares iterative reconvolution (LSIR). The LSIR analyses employ a nonlinear least-squares iterative procedure (Grinvald & Steinberg, 1974) that uses either the Powell search algorithm (Fletcher & Powell, 1963; Himmelblau, 1972) or the Marquardt algorithm (Marquardt, 1963; Bevington, 1969) to determine the values of parameters. In one method, the amplitudes and lifetimes are first determined for the total fluorescence decay, $I(t)$. The difference decay, $D(t)$, is then expressed as a sum of exponential terms whose amplitudes and decay times are functions of the total and anisotropy decay lifetimes and amplitudes [recall that $D(t) = r(t)I(t)$]. The parameters of the anisotropy decay are then fit by holding the fluorescence decay parameters constant. In the second method, the individual vertical and horizontal decays are fit with simultaneous optimization of the fluorescence decay and anisotropy decay parameters (Cross & Fleming, 1984). In either case, the $r(t)$ decays are fit to sums of one, two, or three exponential terms

$$r(t) = \sum_i r_i \exp(-t/\phi_i) \quad (2)$$

where r_i is the amplitude of the decay characterized by the correlation time ϕ_i and $\sum r_i = r_0$, the value of the probe anisotropy at zero time. An adequate fit was determined by evaluating χ^2 and by examining plots of the residuals, defined as the difference between the calculated and the experimental curve at each channel. A fit to $r(t)$ was considered adequate if the residuals plot appeared random. The total fluorescence decay was fit to three or four lifetime components in most anisotropy decay analyses. Studies of the decay of the total intensity in these proteins (Ludescher et al., 1985) have demonstrated that three or sometimes even four exponential terms are required for a complete description. The values of the anisotropy parameters are not appreciably affected by the number of lifetime terms in the fluorescence decay so long as enough terms are used that there is a reasonable fit to the total decay data.

The phenomenologial decay constants (ϕ's) of eq 2 can be related to physical correlation times by assuming that each term in the description of the anisotropy decay corresponds to a different decay mode with a characteristic decay time. Consider the case in which the anisotropy decay is fit by three exponentials. We rank the decay times from smallest to largest. Then ϕ_1, the smallest decay time, actually represents a harmonic sum of the physical decay constants

$$1/\phi_1 = 1/\phi_I + 1/\phi_S + 1/\phi_P \quad (3)$$

where ϕ_I describes the fast rotation of the fluorophore, ϕ_S describes the larger scale segmental motion of some part of the protein containing the fluorophore, and ϕ_P describes the rotation of the whole particle. The corresponding expression for ϕ_2 is

$$1/\phi_2 = 1/\phi_S + 1/\phi_P \quad (4)$$

ϕ_P may itself be a composite correlation time that represents two or more different motional processes. The longest motion time corresponds to unrestricted motion such as particle tumbling. The amplitude of this term (r_p) is the residual anisotropy remaining after all faster motions have ceased. The residual anisotropy can be related, in a model-dependent way, to the semiangle (θ_c) of a cone in which the fluorophore transition dipole freely wobbles (Kinosita et al., 1977; Lipari & Szabo, 1980):

$$r_p/r_0 = \{\cos(\theta_c)[1 + \cos(\theta_c)]\}/4 \quad (5)$$

These motional amplitudes can also be analyzed in a model-independent way by simply inverting the general expression for the anisotropy

$$r_p/r_0 = \langle[3\cos^2(\psi) - 1]/2\rangle^2 \quad (6)$$

to obtain a value for the root mean square cos (ψ). The value of ψ obtained directly from this equation corresponds to a δ-function angular distribution of the transition dipole angle about a symmetry axis [$\rho(\theta) = \delta(\theta - \psi)$]. For the case of a uniform distribution within a cone [$\rho(\theta)$ = constant, $\theta < \theta_c$] we obtain eq 5. The angles θ_c (cone distribution) of eq 5 and ψ (δ-function distribution) of eq 6 are, of course, numerically related. For $\theta_c = 10$, 20, and 30°, $\psi = 7$, 14, and 21°, respectively. The application of any such simple model to the motions of tryptophan in a protein is only approximate but gives a qualitative idea of the range of motions involved for an observed anisotropy decrement.

Rotational Correlation Times. The rotational correlation time of a sphere, $V_h\eta/RT$, was used to evaluate ϕ_P for spheres equivalent in mass to PLA_2, $ProPLA_2$, $PLA_2/C_{16}PN$, and the $C_{16}PN$ micelle. The volume was calculated from the molecular weight and the partial specific volume for each species. Molecular weights of 13 800 and 14 600 were used for PLA_2 and $ProPLA_2$, respectively. The molecular weight of $PLA_2/C_{16}PN$ is temperature dependent and the values used in the calculation [98 000 (8 °C), 84 000 (20 °C), and 60 000 (40 °C)] were estimated from a least-squares fit to the gel filtration values at 15, 25, and 35 °C reported by Soares de Araujo et al. (1979). For the molecular weight of the pure detergent micelle we have used the value at 25 °C determined by Soares de Araujo et al. (1979) from light scattering (90 000). The partial specific volumes used in the calculation were (in cm^3/gm) 0.707 (proteins) and 0.98 (detergent micelle) and for the complex at different temperatures, 0.92 (8 °C), 0.90 (20 °C), and 0.87 (40 °C). The values for the complex were calculated from the weight percent protein and lipid in the complex at each temperature and the partial specific volumes of the pure components (Hille et al., 1981).

RESULTS

Temperature Dependence of the Steady-State Anisotropy. The reciprocal of the steady-state anisotropy, $1/\langle r\rangle$, of Trp-3 in $ProPLA_2$, PLA_2, and the $PLA_2/C_{16}PN$ complex is plotted versus the ratio of temperature to viscosity (T/η) in Figure 2. In this experiment the effect of viscosity on the anisotropy, collected with 300-nm excitation and 340-nm emission, was studied by changing the temperature. $\langle r\rangle$ was substantially lower for $ProPLA_2$ than for PLA_2 at all temperatures measured. Given that the mean fluorescence lifetime for the zymogen is similar to or less than that of the enzyme (Ludescher et al., 1985), this suggests that there is a larger amplitude of motion for the tryptophan in the larger proenzyme. The reciprocal of the y intercept of the plot of $1/\langle r\rangle$ versus T/η gives an estimate of the effective initial anisotropy, $(r_0)_{eff}$. The magnitude of $(r_0)_{eff}$ is a measure of the residual anisotropy that remains at times longer than rapid internal motions. From the plots in Figure 2, $(r_0)_{eff}$ is approximately 0.19 for $ProPLA_2$ and 0.24 for PLA_2. This confirms the conclusion that the lower value of $\langle r\rangle$ for the zymogen is due to a larger amplitude for internal motions of the tryptophan in the protein. At the

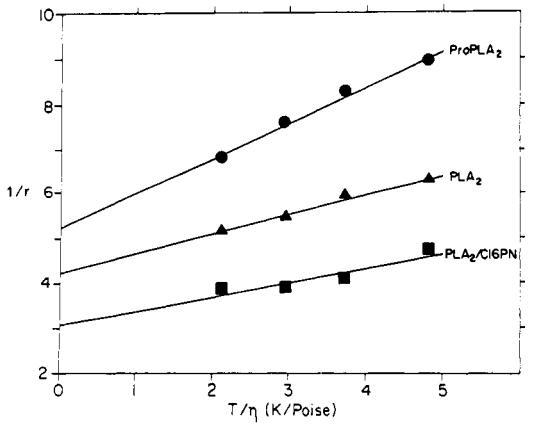

FIGURE 2: Perrin plot of the temperature dependence of the steady-state anisotropy of Trp-3 in $ProPLA_2$, PLA_2, and the $PLA_2/C_{16}PN$ complex. The anisotropy was measured at 8, 20, 29, and 40 °C. The reciprocal of the y intercept is a measure of $(r_0)_{eff}$ (see text). $(r_0)_{eff}$ is 0.19 for $ProPLA_2$, 0.24 for PLA_2, and 0.33 for $PLA_2/C_{16}PN$. Excitation was at 300 nm (4-nm slits) and emission at 340 nm (8-nm slits).

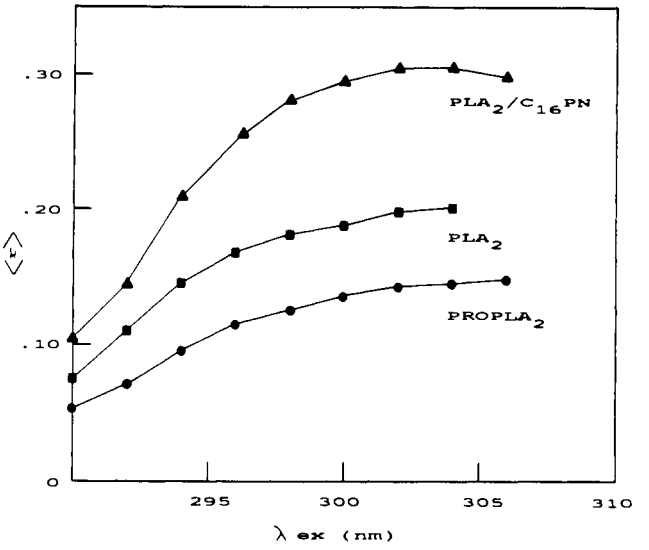

FIGURE 3: Variation of the steady-state anisotropy of PLA_2, $ProPLA_2$, and the $C_{16}PN/PLA_2$ complex. The excitation bandpass was 2 nm; emission was at 350 nm with a bandpass of 16 nm (20 °C).

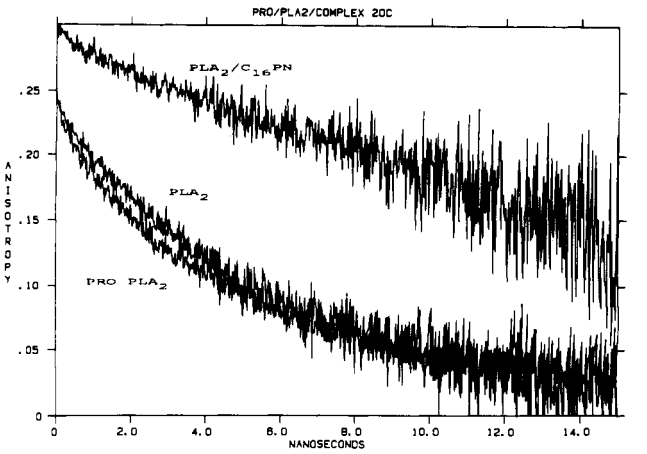

FIGURE 4: Anisotropy decays of Trp-3 in $ProPLA_2$, PLA_2, and the $PLA_2/C_{16}PN$ complex at 20 °C. The curves are calculated point by point directly from the collected parallel and perpendicular decay transients: $r(t) = [I_{vv}(t) - I_{vh}(t)]/[I_{vv}(t) + 2I_{vh}(t)]$. Time zero is the point where the machine response function begins to rise. The excitation wavelength was 300 nm. The emission was collected through a Corning 7-60 broad-band interference filter (310–390-nm transmission, 350-nm maximum).

excitation wavelength of these measurements, r_0 for tryptophan is approximately 0.30[3] (Valeur & Weber, 1977). Since $(r_0)_{eff}$ is lower than 0.30 for both proteins, it appears that Trp-3 has appreciable mobility in these proteins and that the amplitude of the fast motion(s) is larger in $ProPLA_2$ than in PLA_2.

This analysis assumes that the amplitude of the fast internal motion, $r_0 - (r_0)_{eff}$, is independent of temperature. This condition is not expected to hold in general and, although it is consistent with the linearity of the plots of Figure 2, the validity of this assumption is difficult to establish with a limited range of temperature or viscosity. However, the time-resolved measurements presented below are also consistent with a temperature-independent amplitude for the fast motion.

When PLA_2 binds to $C_{16}PN$ micelles, the tryptophan steady-state anisotropy increases from 0.183 to 0.257 at 20 °C. This increase is due in part to a larger rotational correlation time for the complex; the particle molecular weight changes from 13800 to 84000 when the $PLA_2/C_{16}PN$ complex forms (Soares de Araujo et al., 1979). A change in internal dynamics may also contribute to the larger value of $\langle r \rangle$. The increase in $(r_0)_{eff}$ from 0.24 to 0.32 when the enzyme binds to $C_{16}PN$ micelles indicates that the local motion of the tryptophan is sensitive to the formation of a lipid complex. Since $(r_0)_{eff}$ for the tryptophan in $PLA_2/C_{16}PN$ is close to the value expected for a completely immobilized fluorophore (0.30), it is possible that there is little internal rotational motion of Trp-3 in the complex. This is confirmed by the time-dependent analysis given below.

It is conceivable that some (or all) of the difference in the steady-state anisotropy for PLA_2, $ProPLA_2$, and the $C_{16}PN$ complex observed with excitation at 300 nm is due to differences in the value of the intrinsic anisotropy, r_0, at this wavelength due to the shift in the absorption spectrum (Valeur & Weber, 1977; Weber, 1960). In order to test this point, the variation of the average (static) anisotropy, $\langle r \rangle$, was determined for each sample as a function of excitation wavelength (Figure 3). A very similar monotonic decrease in $\langle r \rangle$ was observed as the excitation wavelength was decreased from 306 to 290 nm. We conclude from this that spectral differences are not the origin of the significant differences between the values of $\langle r \rangle$ of the tryptophan fluorescence in these three environments.

Time-Resolved Anisotropy of Trp-3. The time-resolved anisotropy decays of Trp-3 in $ProPLA_2$, PLA_2, and $PLA_2/C_{16}PN$ at 20 °C are plotted in Figure 4. The curves are calculated directly from the parallel and perpendicular decay transients. The machine response function is fast enough (fwhm of ca. 100 ps) that only the initial portion of the decay contains appreciable convolution artifacts (Papenhuijzen & Visser, 1983). We can thus make some qualitative conclusions from an examination of the raw data. First, the slopes of the long decay for $ProPLA_2$ and PLA_2 are similar, while the decay of the complex is much slower. Second, the amplitude of the fast decay, determined by extrapolating the slowly decaying linear region of the anisotropy curve back to zero time and subtracting this value from $r_0 = 0.30$, is much larger for $ProPLA_2$ and PLA_2 than for the lipid complex. Third, there appears to be a significant difference between the zymogen and the processed enzyme in the intermediate time region, with the zymogen having a higher anisotropy throughout this region.

[3] A determination of r_0 for *N*-acetyltryptophanamide in propylene glycol using the apparatus used for these time-resolved protein studies results in a value of $r_0 = 0.29$–0.32 for the same excitation and emission conditions.

Table I: Analysis of the Anisotropy Decay of Prophospholipase A_2 at 20 °C[a]

app/rng[b]	τ/ϕ[c]	r_1	ϕ_1 (ps)	r_2	ϕ_2 (ns)	r_p	ϕ_p (ns)	χ^2	r_0
PMT/30	4/3	0.14 ± 0.04	120 ± 30	0.08 ± 0.01	2.5 ± 0.2	0.16 ± 0.01	8.0 ± 0.2	1.50	0.38 ± 0.06
	3/3	0.11 ± 0.07	170 ± 70	0.09 ± 0.01	2.8 ± 0.3	0.15 ± 0.01	8.3 ± 0.3	1.61	0.35 ± 0.09
	4/2			0.07 ± 0.00	1.3 ± 0.7	0.19 ± 0.00	7.2 ± 0.1	1.61	0.26 ± 0.01
	3/2			0.08 ± 0.00	2.2 ± 0.1	0.17 ± 0.00	7.9 ± 0.2	1.63	0.25 ± 0.01
MCP/40	4/3	0.06 ± 0.08	76 ± 62	0.06 ± 0.00	1.3 ± 0.1	0.17 ± 0.00	7.5 ± 0.1	1.11	0.29 ± 0.09
	3/3	0.11 ± 0.05	81 ± 30	0.06 ± 0.00	1.6 ± 0.2	0.17 ± 0.00	7.7 ± 0.2	1.24	0.33 ± 0.05
	4/2			0.06 ± 0.00	1.1 ± 0.1	0.18 ± 0.00	7.3 ± 0.1	1.12	0.24 ± 0.00
	3/2			0.06 ± 0.00	1.1 ± 0.1	0.18 ± 0.00	7.3 ± 0.1	1.28	0.24 ± 0.00
	4/1					0.21 ± 0.00	5.9 ± 0.0	1.60	0.21 ± 0.00
	3/1					0.21 ± 0.00	5.9 ± 0.0	1.75	0.21 ± 0.00
MCP/20	4/3	0.12 ± 0.05	87 ± 28	0.08 ± 0.01	2.2 ± 0.3	0.16 ± 0.01	8.2 ± 0.5	1.05	0.36 ± 0.07
	3/3	0.14 ± 0.06	82 ± 26	0.08 ± 0.01	2.2 ± 0.3	0.16 ± 0.01	8.2 ± 0.5	1.08	0.37 ± 0.08
	4/2			0.06 ± 0.00	1.0 ± 0.1	0.19 ± 0.00	7.2 ± 0.1	1.09	0.25 ± 0.00
	3/2			0.06 ± 0.00	1.1 ± 0.1	0.19 ± 0.00	7.2 ± 0.1	1.18	0.25 ± 0.00
	4/1					0.23 ± 0.00	5.8 ± 0.0	1.41	0.23 ± 0.00
	3/1					0.23 ± 0.00	5.8 ± 0.0	1.44	0.23 ± 0.00

[a] Excitation at 300 nm; emission collected through a broad-band filter (Corning 7-60; 310–390-nm transmission, maximum at 350 nm). [b] Apparatus/time range. PMT = photomultiplier detection; MCP = microchannel plate detector. The full-scale time range is 20, 30, or 40 ns as indicated. [c] Number of lifetime components (τ) used in the analysis of the total decay and the number of decay components (ϕ) used in the analysis of the anisotropy decay.

Table II: Analysis of the Anisotropy Decay of Phospholipase A_2[a]

app/rng	τ/ϕ	r_1	ϕ_1 (ps)	r_p	ϕ_p (ns)	r_0	χ^2
MCP/40	4/2	0.06 ± 0.02	114 ± 28	0.24 ± 0.00	6.3 ± 0.0	0.31 ± 0.02	1.095
	4/1			0.25 ± 0.00	6.1 ± 0.0	0.25 ± 0.00	1.169
MCP/20	4/2	0.10 ± 0.06	76 ± 30	0.24 ± 0.00	6.1 ± 0.0	0.34 ± 0.06	1.053
	4/1			0.24 ± 0.00	6.0 ± 0.0	0.24 ± 0.00	1.098
MCP/10	4/2	0.03 ± 0.01	220 ± 53	0.24 ± 0.00	6.4 ± 0.1	0.27 ± 0.01	1.107
	4/1			0.24 ± 0.00	6.1 ± 0.0	0.24 ± 0.00	1.165

[a] Same conditions and notations as for Table I.

Table III: Anisotropy Decay Parameters for Trp-3 in $ProPLA_2$ and PLA_2 at 8, 20, and 40 °C[a]

sample	T (°C)	r_1	ϕ_1 (ps)	r_2	ϕ_2 (ns)	r_p	ϕ_p (ns)	r_0
$ProPLA_2$	8	0.06[b]	40 ± 7	0.030 ± 0.003	1.7 ± 0.3	0.21 ± 0.04	8.4 ± 0.1	
	20	0.07 ± 0.03	180 ± 80	0.08 ± 0.01	2.7 ± 0.4	0.16 ± 0.01	8.2 ± 0.4	0.30
	20*	0.06 ± 0.08	76 ± 62	0.06 ± 0.00	1.3 ± 0.1	0.17 ± 0.00	7.5 ± 0.1	0.29
	40	0.08 ± 0.16	100 ± 30	0.03 ± 0.03	0.6 ± 0.4	0.19 ± 0.01	3.4 ± 0.1	0.30
PLA_2	8	0.1 ± 0.4	100 ± 20			0.247 ± 0.001	9.95 ± 0.08	0.35
	20	0.057[c]	180 ± 40			0.243 ± 0.001	6.97 ± 0.04	
	20*	0.06 ± 0.02	114 ± 28			0.240 ± 0.001	6.35 ± 0.05	0.31
	40	0.07 ± 0.11	100 ± 100			0.222 ± 0.001	3.32 ± 0.02	0.29

[a] Same conditions as in Table I. The data were obtained with the PMT apparatus except for the 20 °C case marked with an asterisk, which is the result of an analysis of data obtained with the MCP device. [b,c] The values are obtained by subtracting the sum of the more accurately determined values of the longer time components from 0.3. The values of r_1 obtained for these cases are clearly too large: (*b*) $r_1 = 0.5 \pm 0.9$; (*c*) $r_1 = 0.5 \pm 0.1$.

All of these conclusions are confirmed by quantitative curve-fitting analyses.

Trp-3 Dynamics in $ProPLA_2$ and PLA_2. The results of a detailed analysis of the anisotropy decay of Trp-3 in $ProPLA_2$ at 20 °C by least-squares iterative reconvolution (LSIR) are presented in Figure 5a and Table I. The bottom curves are plots of the undeconvoluted anisotropy decay calculated directly from the parallel and perpendicular decay transients. The convoluted fit functions are also plotted (smooth curves through the data). The upper curves in each panel show the modified residuals for the individual parallel and perpendicular decay transients. A similar analysis of the decay of Trp-3 anisotropy in PLA_2 at 20 °C is plotted in Figure 5b.

A detailed numerical analysis was made of much of the data. An example is given in Table I. This case of $proPLA_2$ at 20 °C is one of the most complex situations observed and illustrates the reasoning used. The individual parallel and perpendicular decay data were fit simultaneously with optimization of both the fluorescence lifetime decay and anisotropy decay parameters. In this way the χ^2 values obtained represent the overall fit of the entire model to the data (Cross & Fleming, 1984). The results for both three- and four-component lifetime decay models and one-, two-, and three-component anisotropy decay models are shown. Data for both the PMT and MCP systems are shown. It is evident that the number of components used in the lifetime analysis (three or four) has only a minor effect on the extracted anisotropy parameters in most cases.

Table II presents a similar analysis of several sets of data obtained for PLA_2 at 20 °C. Attempts to fit these data with three correlation times resulted in two identical correlation times, zero amplitudes, or zero-divide errors.

The fit parameters from LSIR analysis of Trp-3 anisotropy decays in $ProPLA_2$ and PLA_2 at 8, 20, and 40 °C are listed in Table III. The sum of the preexponential terms, r_0, is included for each case. Except in two instances where r_1 is unreasonably large, the fit r_0 values are close to the expected value of 0.3. This demonstrates that we are resolving all of the motion of Trp-3 in these proteins.

The long-time decay terms (r_p and ϕ_p) presumably correspond to isotropic rotation of the proteins. The variation of this relaxation time with η/T is shown in Figure 6. The rotational diffusion times calculated from the Stokes–Einstein equation for a sphere equivalent in volume to these proteins

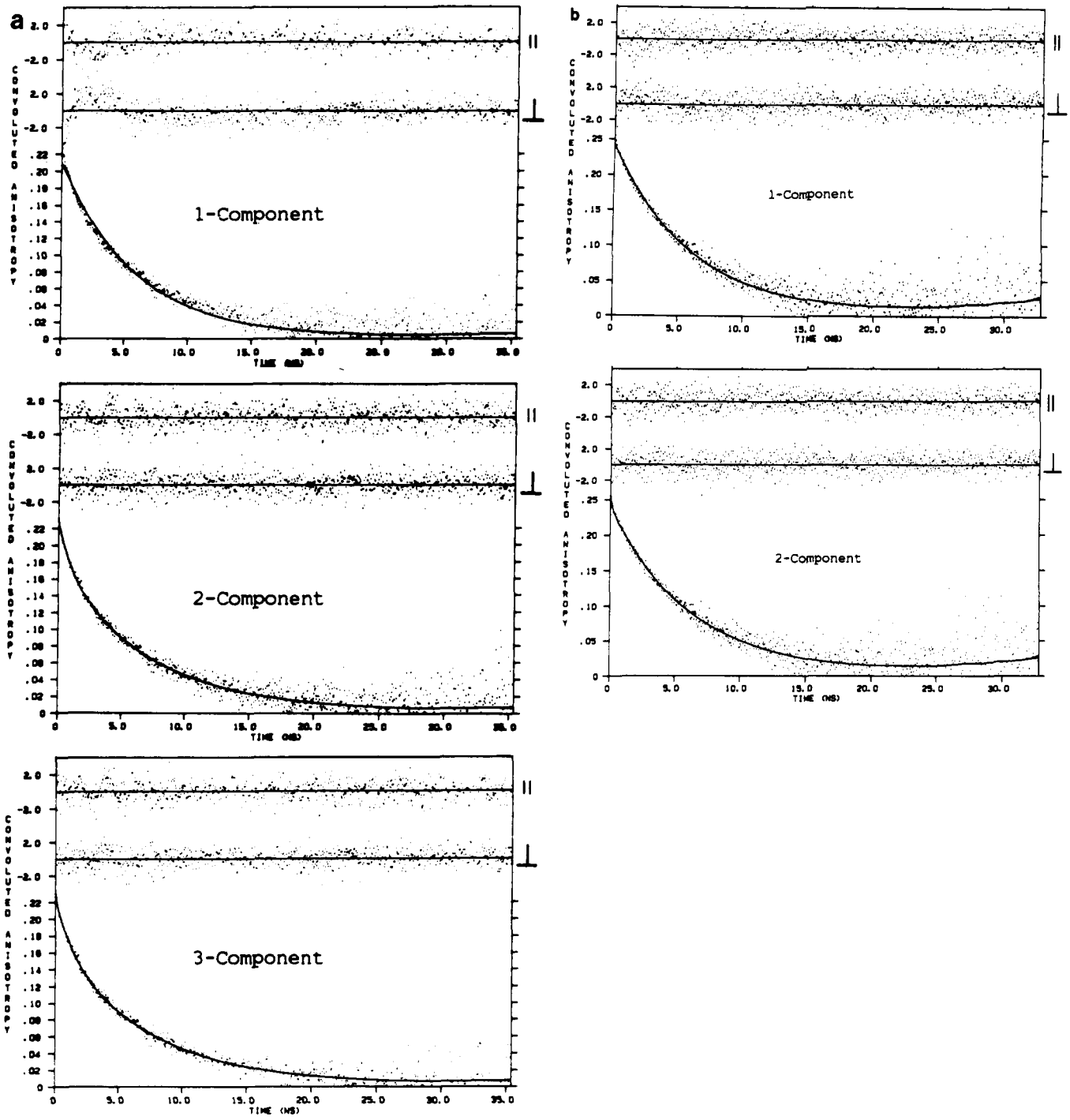

FIGURE 5: LSIR analysis of the anisotropy decay of Trp-3 in $ProPLA_2$ (a) and PLA_2 (b) at 20 °C. The noisy decays are the undeconvoluted anisotropy decays (calculated as in Figure 3). (a) One-, two-, and three-component exponential component functions fit to the $ProPLA_2$ anisotropy decay convoluted with the machine response function are plotted as smooth curves through the data. The modified residuals for the individual parallel and perpendicular decay transients are shown at the top of each panel. (b) One- and two-exponential fits to the PLA_2 anisotropy decay are plotted through the data; the residuals are also plotted. For both cases the excitation was at 300 nm, and emission was collected through a Corning 7-60 band-pass filter (310–390 nm, maximum at 350 nm).

are also plotted in Figure 6.[4] The measured correlation times for both proteins are larger than the calculated values at each temperature. This is to be expected since the calculated values are based on the unhydrated molecular weights for spherical particles. The values of ϕ_p for PLA_2 are roughly linear with η/T, but the values for $ProPLA_2$ deviate significantly. The reason for this behavior is not clear.

The influence of glycerol on the dynamics of Trp-3 in $ProPLA_2$ at 20 °C is illustrated in Figure 7. The anisotropy decay is plotted for glycerol concentrations of 0, 44, and 57 wt %. The slope of the decay is obviously affected by the increased solution viscosity. In the inset to Figure 7 the long correlation times are plotted versus solution viscosity. The excellent linear relation demonstrates that this correlation time corresponds to the rotation of the entire protein. The variation of ϕ_p vs η/T is essentially the same for Figure 6 (where temperature was varied) and Figure 7 (where the viscosity was

[4] The molecular volume that we calculate from the protein dimensions quoted in Allegrini et al. (1985) results in a rotational correlation time of 4 ns, in very close agreement with the value obtained from the partial specific volume and molecular weight as used here.

Table IV: Fit Anisotropy Decay Parameters for Trp-3 in $PLA_2/C_{16}PN$ and tPnA in $C_{16}PN$ Micelles at 8, 20, and 40 °C[a]

sample	T (°C)	r_1	ϕ_1 (ps)	r_2	ϕ_2 (ns)	r_p	ϕ_p (ns)	ϕ_c[b] (ns)	r_0
$PLA_2/C_{16}PN$	8	0.02 ± 0.04	200 ± 20			0.286 ± 0.001	27.6 ± 0.3	53	0.31
	20	0.024[c]	70 ± 70			0.276 ± 0.001	16.1 ± 0.1	33	
	20*	0.023 ± 0.004	203 ± 48			0.291 ± 0.001	21.7 ± 0.3	33	0.31
	40	0.02 ± 0.56	40 ± 15			0.268 ± 0.001	6.8[d]	13	0.29
$tPnA/C_{16}PN$	8	0.133 ± 0.001	240 ± 10	0.06 ± 0.01	1.25 ± 0.01	0.204 ± 0.001	29.6 ± 0.1	52	0.40
	20	0.151 ± 0.001	150 ± 10	0.08 ± 0.01	0.74 ± 0.01	0.171 ± 0.001	15.4 ± 0.1	39	0.40
	40	[e]		0.18 ± 0.01	0.29 ± 0.01	0.151 ± 0.001	6.7 ± 0.1	22	0.33

[a] Tryptophan excitation at 300 nm; emission collected through a broad-band filter (310–390 nm, maximum at 350 nm). Parinaric acid excitation at 300 nm; emission collected through a Corning 0-52 long pass filter (transmission cutoff at 350 nm). All data were obtained with the photomultiplier detector except for the 20 °C experiment marked with an asterisk. [b] Calculated particle correlation time for an unhydrated sphere of the same volume. [c] This value is an estimate of the amplitude of the rapid component determined by subtracting the more accurately determined value of r_p from 0.3. The fit value of $r_1 = 0.1 \pm 0.2$. [d] This value is an underestimate because of downward curvature in the anisotropy decay. [e] LSIR analysis finds only two exponentials. The low value of r_0 indicates that a fast-decay component is not being resolved.

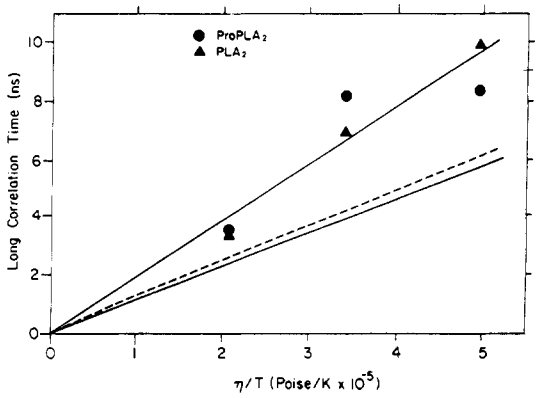

FIGURE 6: Particle rotational correlation times for $ProPLA_2$ (●) and PLA_2 (▲) as listed in Table II. The lines at the bottom show the behavior expected for unhydrated spheres of the equivalent volume. The dashed line is for $ProPLA_2$; the solid line is for PLA_2.

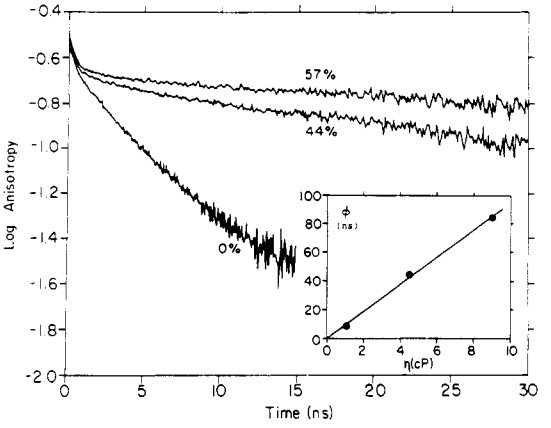

FIGURE 7: Effect of glycerol on the anisotropy decay of Trp-3 in $ProPLA_2$ at 20 °C. The decays are in 0, 44, and 57 wt % glycerol (lowest to highest). The inset shows the dependence of the particle rotational correlation time (ϕ_P) on the solution viscosity. Excitation was at 300 nm, and emission was through a broad-band emission filter (Corning 7-60).

varied by addition of glycerol). This demonstrates that the longest decay component of the anisotropy indeed represents overall rotation of the protein.

Trp-3 Dynamics in the $PLA_2/C_{16}PN$ Complex. The results of LSIR analysis of the anisotropy decay of Trp-3 in $PLA_2/C_{16}PN$ micelles at 8, 20, and 40 °C are listed in Table IV. The analysis finds two exponentials for the decay at each temperature. The sum of the preexponentials is found to be close to 0.3, again indicating that we are resolving all of the motion. The amplitude associated with particle decay (r_p) in the complex is considerably higher than the corresponding amplitude in PLA_2 (compare Tables II and III). This clearly shows that the amplitude of the fast decay decreases upon complex formation.

At 8 and 20 °C two exponentials can be considered an adequate fit to the anisotropy decay. The decay behavior at 40 °C, however, is unusual and cannot be described by a simple sum of exponentials. In this case $r(t)$ curves downward at long time; i.e., the slope of the curve becomes more negative at longer time. This behavior is not an instrumental artifact. This effect is reproducible, is not seen in PLA_2 decays, and appears only when PLA_2 forms a complex with $C_{16}PN$. This behavior is probably due to population heterogeneity in the fluorescence lifetime of the complex and a correlation between the fluorescence lifetime and the rotational correlation time. Similar behavior has been seen in other systems (Ludescher, 1984a,b) and is discussed elsewhere (Ludescher et al., 1987; Hudson et al., 1986, 1987).

The correlation times for isotropic rotation of the $PLA_2/C_{16}PN$ complex (Table IV) are smaller than the values predicted from the Stokes–Einstein equation. These differences are even more significant because the calculations assume an unhydrated spherical particle and are thus *minimum* values. Since the detergent micelle is not a rigid particle, the lower correlation time may be due to a slow internal motion of the chromophore in the micelle. Such a motion would not be detected separately from overall particle rotation if it is isotropic, i.e., unconstrained, and on the same time scale as the particle rotation. This is in contrast to the constrained internal motions seen in $ProPLA_2$ and PLA_2. It is straightforward (see eq 4 under Materials and Methods) to calculate the correlation time of this postulated internal motion from the measured values of ϕ_p and the calculated particle rotational correlation times. These values range from about 60 ns at 8 °C to about 14 ns at 40 °C. The possibility of a slow internal motion of Trp-3 in the $PLA_2/C_{16}PN$ micelles is supported by anisotropy decay measurements for the polyene fatty acid fluorophore *trans*-parinaric acid (Sklar et al., 1977; Hudson & Cavalier, 1987) in pure $C_{16}PN$ micelles. The parameters of the anisotropy decays at 8, 20, and 40 °C are listed in Table IV. The longest correlation times detected by this probe are very similar to the values observed for the $PLA_2/C_{16}PN$ complex and considerably less than the values calculated for a rigid sphere with the micellar volume.

The zymogen does not bind to micelles of *n*-alkylphosphocholines. The anisotropy decay of $ProPLA_2$ in the presence of 5 mM $C_{16}PN$ at 20 °C requires a three-exponential description. The overall protein correlation time, ϕ_p, is unchanged by the presence of the detergent, demonstrating that a protein/micelle complex is not formed. The amplitude of the intermediate motion (r_2), however, decreases by more than half. The reason for this is not clear but could involve binding of monomeric $C_{16}PN$ to the zymogen. This binding is expected given that the zymogen is enzymatically active toward monomeric phospholipids.

The anisotropy behavior observed for *trans*-parinaric acid in $C_{16}PN$ micelles is quite similar to that observed for the tryptophan residue of $ProPLA_2$. The fact that the values of r_0 obtained from fits to these data at 8 and 20 °C are precisely equal to the known value of 0.4 for *trans*-parinaric acid (Hudson & Cavalier, 1987), which is also the theoretical maximum, confirms the reliability of the data obtained with this apparatus and the method of analysis used. This indicates that variations in the value of r_0 observed for protein tryptophan fluorescence represent a lack of resolution of rapid internal reorientational motion.

Discussion

The analysis of the anisotropy decay for the tryptophan residue of PLA_2 (Table II) shows that a single-exponential form results in a reasonable value of χ^2 but a low value of r_0. Analysis with a double-exponential form results in only a small decrease in χ^2 but improves r_0 considerably. Inclusion of this second-exponential component has little effect on the amplitude or relaxation time for the slower (overall rotation) motion, and thus the interpretation of the long-time behavior of the anisotropy decay is unaffected by the inclusion of a term representing the rapid motion.

The correlation times for the fast motion of Trp-3 in PLA_2 at 20 °C obtained from a double-exponential analysis of the anisotropy decay appear to be in the 75–220 ps range; the mean value obtained with five independent determinations was 134 ± 26 ps. The statistical uncertainty on any one determination is rather high, however, and this number can only be considered an estimate. The angular extent of the fast motion of Trp-3 in PLA_2 can be reliably estimated from the values of the anisotropy decrement associated with this fast motion. The values of r_p determined from the tryptophan anisotropy decays range from 0.22 to 0.25,[5] in excellent agreement with the value of $(r_0)_{eff}$ of 0.24 determined from the temperature–viscosity variation of the steady-state polarization (Figure 2). The temperature dependence of r_p, although small, is in the expected direction, and the statistical errors are small. We therefore believe that these values of r_p are reasonably precise and that $r_0 - r_p$ accurately reflects the amplitude of internal motion of the tryptophan residue. We can convert these values into a (model-dependent) angular extent using eq 5 and an r_0 of 0.3. At 20 °C Trp-3 in PLA_2 can rotate through a cone of semiangle (θ_c) of 21° when PLA_2 is free in solution. This angular range is substantially independent of temperature being 20–21° at 8 °C and 25° at 40 °C.

The range of angular motion observed for the tryptophan residue of PLA_2 is in agreement with a static model building calculation presented in Figure 8. This calculation is based on the 1.7-Å resolution structure of the bovine enzyme (Dijkstra et al., 1983). The graphics program FRODO (Jones, 1978) running on MMS-X hardware was used to rotate Trp-3 about its C_β–C_γ bond (with all other angles held fixed) until van der Waals contact distances were approached. This rotation preserves the indole N–H hydrogen bond present in the X-ray structure and causes a large reorientation of the indole transition dipole (Yamamoto & Tanaka, 1972). Rotations of +20° and −25° (relative to the X-ray-determined equilibrium structure) were possible before van der Waals contacts were encountered. This range of 45° compares well with the value of 42° deduced from the fluorescence measurements. Furthermore, a "static protein" model of this motion is consistent with the temperature independence of the range of this motion. The relatively rigid nature of the protein is reasonable given its extensive disulfide cross-linking. Thus, we conclude that the amplitude of the fast internal motion of Trp-3 of PLA_2 makes sense in terms of the structure of this protein.

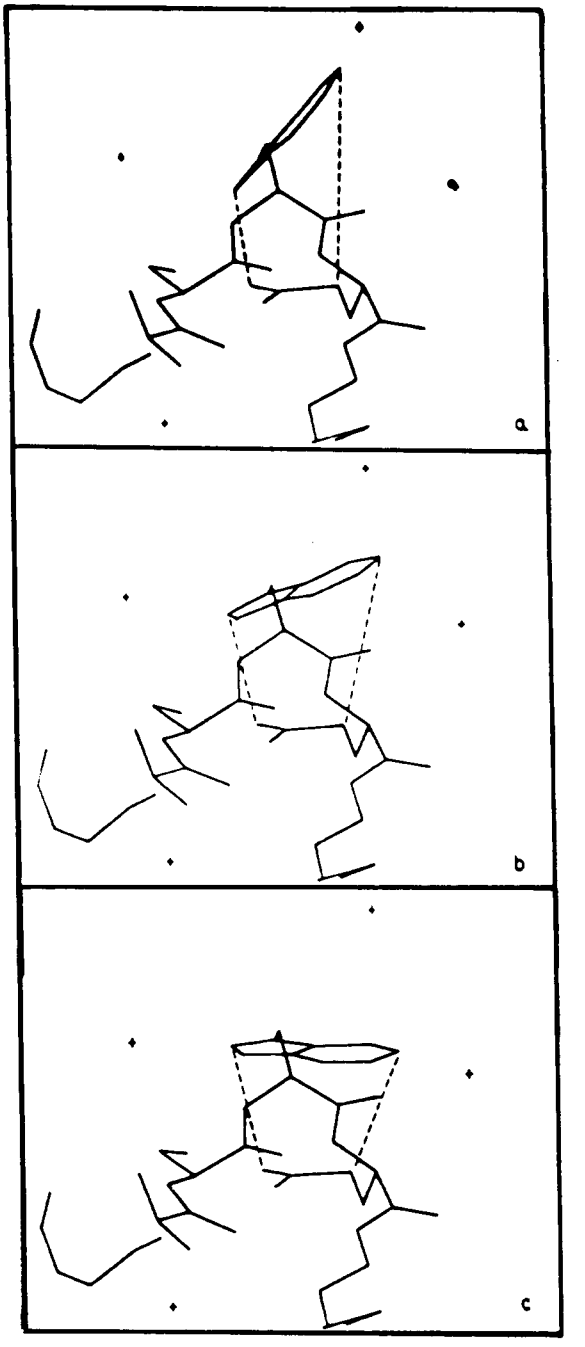

FIGURE 8: Structure of the Trp-3 residue and its immediate environment in bovine phospholipase A_2. In panel a the Trp-3 ring has been rotated clockwise about the C_β–C_γ bond until van der Waals contact is reached. Panel b shows the unrotated structure observed for the crystal. Panel c is the same as (a) but with rotation in the opposite direction. The small crosses are crystallographically determined water molecules.

The binding of PLA_2 to $C_{16}PN$ micelles decreases the amplitude of the fast rotational motion of Trp-3 (compare Tables III and IV). The values obtained for r_p from the time-resolved measurements (0.27–0.29) are essentially temperature independent and in reasonable agreement with the value of $(r_0)_{eff}$

[5] The mean and standard deviation of the amplitude of the longest correlation time motion obtained from four independent experiments conducted with the MCP system were 0.240 ± 0.001 for analyses in which two anisotropy relaxation times were employed and 0.244 ± 0.001 when analyzed by using only a single relaxation time.

of 0.3 obtained from the steady-state polarization measurements for this complex. The small decrement of r from the value of 0.3 corresponds to a value of $\theta_c = 14°$ for PLA_2 in the complex, compared to a value of 21° for PLA_2 in solution. Thus, PLA_2 binding to $C_{16}PN$ seems to decrease the conformational flexibility of Trp-3. The molecular interactions that cause this immobilization are either protein–protein or protein–lipid. Since the binding transfers the tryptophan into a hydrophobic environment (Van Dam-Mieras et al., 1975; Ludescher et al., 1985), we conclude that lipid–protein interactions are probably responsible. Complex formation may involve a local conformational change at the N-terminus that swings the tryptophan away from the face of the protein to interdigitate with the acyl chains of the micellar lipids.

The particle rotational correlation times measured for the $PLA_2/C_{16}PN$ micelle are less than the calculated values for an equivalent sphere. This result is also found for the pure $C_{16}PN$ micelle probed with *trans*-parinaric acid. There is ample evidence that the molecular weights of the $C_{16}PN$ and $PLA_2/C_{16}PN$ micelles used to calculate the ϕ_P values are accurate. The $PLA_2/C_{16}PN$ molecular weights determined by light scattering (Donne-Op den Kelder et al., 1981) and gel filtration (Soares de Araujo et al., 1979) are in good agreement. The molecular weight of $C_{16}PN$ micelles has been determined from light scattering (Soares de Araujo et al., 1979). The angular dependence of the scattering intensity indicates that both the $C_{16}PN$ and $PLA_2/C_{16}PN$ micelles are monodisperse. Thus, the discrepancy between the calculated and observed values cannot be due to errors in the molecular weights. A possible explanation for the shorter than expected rotational correlation times is that there is an isotropic "slow" internal motion in the detergent micelle. The absence of any specific molecular details on the nature of lipid motions in micelles complicates an interpretation (Wennerstrom & Lindman, 1979). Lindblom and Wennerstrom (1979) measured D for various amphiphiles in lyotropic liquid crystals and found values ranging from 2.2×10^{-6} to 5×10^{-8} cm^2 s^{-1}. It is interesting to note that a particle with a diffusion coefficient of 10^{-6} cm^2 s^{-1} diffusing on the surface of a sphere the size of one of these micelles moves through an angle of 57° in 25 ns. Thus, the diffusional interchange of lipid molecules, responsible for translation diffusion, results in rapid reorientational motion for a small spherical particle.

A recent study of the dynamics of deuterium-labeled Trp-3 and Phe-5 in bovine PLA_2 and Trp-3 in porcine PLA_2, deduced from deuterium NMR T_1 and resonance line widths (Allegrini et al., 1985), differs from our results in several respects. Comparison is complicated because analyses of the NMR data were probably based on a single correlation time model, while our results indicate that there is significant internal motion for Trp-3 in PLA_2. These authors determine a correlation time of 10 ns for porcine PLA_2 at 20 °C (adjusted to dilute solution), a value somewhat longer than the value of 7–8 ns we obtain. They interpret this correlation time as being due to overall particle motion and conclude that the protein is internally rigid. From the disappearance of the deuterium NMR signal in the porcine $PLA_2/C_{16}PN$ complex, they estimate that the correlation time is greater than 35 ns. This result for the porcine enzyme is qualitatively consistent with our observations. Allegrini et al. (1985) observed a very narrow resonance for Trp-3 in bovine PLA_2 from which they calculate a correlation time of 10 ps. This extreme difference between two homologous and isostructural proteins is very surprising. We have measured the static anisotropy of the Trp-3 fluorescence for the bovine enzyme and obtain a value of $\langle r \rangle = 0.16$ at 20 °C. The corresponding value for the porcine enzyme is $\langle r \rangle = 0.18$. We conclude that the dynamic behavior for the Trp-3 residues of these proteins is very similar, as expected.

Our results indicate that the tryptophan residue in the zymogen exhibits complex internal dynamics. Both the static and the time-resolved anisotropy demonstrate that Trp-3 has greater freedom of motion in $ProPLA_2$ than in PLA_2. The static anisotropy is lower at all temperatures measured and the extrapolated $(r_0)_{eff}$ is 0.19 compared to 0.24 for PLA_2. This value for the zymogen is very similar to the value of r_p obtained from the time-resolved anisotropy measurements (Table I), increasing our confidence in these results.

The analysis of the rapid internal motion of Trp-3 in the zymogen presented in Table I and Figure 5 clearly demonstrates that more than one exponential component is required to fit the data. When a two-component analysis is employed, the relaxation times obtained are 7.2 and 1.1 ns. The larger value corresponds to overall rotation as discussed above; the smaller value is clearly much longer than the value obtained from the corresponding analysis for PLA_2, where $\phi \approx 130$ ps or almost 10-fold smaller. This clearly demonstrates a dynamic difference between these two proteins. At this level of analysis the time scale of this internal motion is fairly well determined. The value of r_0 obtained (0.24 ± 0.01) is slightly lower than the expected zero-time value. If the same data are analyzed by using a three-component fit, the value of r_0 increases to a value that is somewhat higher than the expected limiting value; the decrease in χ^2 for the three-term fit relative to the two-term fit is small or negligible. An example of the resulting modified residuals is given in Figure 5a. Overall, the three-component fit is not particularly preferable to the two-component fit. The parameter values obtained from the three-component fit are reasonable, however. The value of the shortest relaxation time, $\phi_1 = 94 \pm 11$ ps, is comparable to the value obtained for PLA_2. The value of the intermediate relaxation time is slightly shorter when a new component is included, but it is still much larger than the internal motion time scale. Overall, a three-component analysis is not required for these data, but it is not unreasonable.

Independent of this choice, however, it is clear that Trp-3 in $ProPLA_2$ has more motional freedom than in PLA_2. According to the three-component analysis, the correlation time of the new motional component of $ProPLA_2$ is 1.5–3.5 ns at 20 °C (see eq 4 under Materials and Methods). This correlation time is in the range expected for segmental motion of a portion of the protein containing the tryptophan. Both PLA_2 and $ProPLA_2$ have seven disulfide bonds in a 14 000-dalton protein. Such extensive cross-linking will severely restrict the overall segmental flexibility of the molecule. Since the first disulfide residue is at position 11 and the tryptophan is at position 3, the segmental motion in the zymogen may involve the independent motion of some or all of the first 17 residues (pyroGlu-7 to Lys-10). There are additional structural features that support this interpretation. First, the N-terminal α-helix of both bovine and porcine PLA_2 is anchored to the protein surface in the crystal by extensive hydrogen bonding of the α-NH_3^+ group of Ala-1 (Dijkstra et al., 1981a, 1983). In contrast, the N-terminal amino acid of the zymogen is a pyroglutamic acid, which has no free NH_3^+ amino group. Second, the first 10 amino acids of the bovine zymogen, including Trp-3, are disordered in the crystal (Dijkstra et al., 1982).

A comparison of the crystal structures of bovine $ProPLA_2$ and PLA_2 indicates that the proteins have nearly identical conformations except for two regions that are disordered in

the zymogen (Dijkstra et al., 1982). Besides the N-terminal region from residues −7 to 3 discussed above, residues 62–74, which form a loop between helix D and a strand of the β-sheet (see Figure 1), are visible in the electron density map of the zymogen but are considerably disordered. A comparison of the porcine proteins is not possible because a reliable crystal structure of the porcine zymogen is not yet available. In porcine PLA_2 (Dijkstra et al., 1983) the α-amino group of Ala-1 forms hydrogen bonds to Gln-4, to a water molecule that is hydrogen bonded to residues in the active site, and to the peptide carbonyl of Glu-71 (Asn-71 in the bovine enzyme). Disruption of this hydrogen-bonding network by chemical modification (Slotboom et al., 1978) indicates that it serves to anchor the N-terminal α-helix of PLA_2 in a manner that is essential for the bonding of PLA_2 to lipid–water interfaces. Since Asn-71 is in the disordered loop of the bovine zymogen, the hydrogen bond to Ala-1 may help to stabilize this loop in PLA_2. The N-terminal segmental disorder found in crystalline bovine $ProPLA_2$, which may be either dynamic or static disorder, is shown by these present studies to have a dynamic component. As Dijkstra et al. (1982) have previously suggested, this additional segmental freedom in the zymogen may be an essential element of the lack of $ProPLA_2$ activity toward lipid aggregates.

The regulation of enzyme activity by conformational freedom also seems to underlie the difference in activity of trypsinogen and trypsin (Huber & Bode, 1978; Huber & Bennett, 1983). Trypsinogen is converted to trypsin by cleavage of six residues from the N-terminus. The new N-terminal amino acid, Ile-16, then forms an internal salt bridge with Asp-194 that stabilizes a region of the protein surface called the activation domain. The activation domain includes the specificity pocket of trypsin as well as portions of the active site. The activation of trypsin by proteolytic cleavage thus appears to involve the formation of specific interactions between the new N-terminal residues and the protein itself that stabilize a specific conformation in an otherwise flexible molecule. The zymogen is apparently inactive because substrate binding is hindered due to the conformational flexibility of the activation domain.

A similar mechanism for zymogen activation toward surface catalysis may be operating in phospholipase A_2. Cleavage of the seven amino acids from the N-terminus eliminates conformational states or dynamic flexibility of the zymogen in a region of the molecule that is considered part of the lipid-binding domain (Dijkstra et al., 1981b). We propose that the extensive segmental flexibility that exists in solution may account for the failure of $ProPLA_2$ to bind to neutral lipid aggregates. The extra conformational freedom at the N-terminus may present a significant entropic impediment to complex formation if a specific conformational state is needed for binding. The finding that the amplitude of the fast rotation of PLA_2 decreases in the $C_{16}PN$ complex indicates that, at least for this residue, a rather static structure is achieved upon complex formation. If the decrease in dynamic freedom found for Trp-3 also occurs for other residues, the decrease in configurational entropy for $ProPLA_2$ upon binding may be of sufficient magnitude to prevent complex formation. Recent studies indicate that $ProPLA_2$ can bind to negatively charged micelles (Volwerk et al., 1985). In this case, the electrostatic interaction of the negatively charged lipids with positively charged residues on the surface of $ProPLA_2$ may compensate for any loss of configurational entropy that binding entails.

In summary, these time-resolved anisotropy measurements demonstrate that Trp-3 in the enzyme phospholipase A_2 undergoes appreciable internal mobility on the subnanosecond time scale. When PLA_2 forms a complex with the nonhydrolyzable substrate analogue *n*-hexadecylphosphocholine, the amplitude of this rapid wobble decreases by about half. The low value of the rotational correlation time of the $PLA_2/C_{16}PN$ complex supports a model of the protein/lipid micelle in which the protein undergoes surface translational diffusion on the time scale of the tryptophan fluorescence lifetime. In addition, we show that the anisotropy decay of Trp-3 in the zymogen is more complex than in the processed enzyme. There is an additional rotational motion of intermediate time scale (≈3 ns) that is probably due to the segmental flexibility of the N-terminus of the protein. This additional flexibility at the N-terminus may be related to the inability of the zymogen to bind to neutral lipid/water interfaces.

ACKNOWLEDGMENTS

R.D.L. is especially grateful to Enoch Small and Louis Libertini for extensive technical expertise and patient assistance that was indispensable to the successful completion of this work; he is also thankful for many helpful discussions with Anthony Ruggiero, Duane Flamig, and the late Irvin Isenberg. The use of Peter von Hippel's SLM spectrofluorometer and the help of Jim McSwiggen is greatly appreciated. We also appreciate the assistance provided by Dale Tronrud in the use of the molecular graphics system of Brian Matthew's laboratory. We thank Suzanne Hudson for writing the numerical analysis and plotting computer programs. We also acknowledge the comments of a referee concerning the potential importance of the wavelength dependence of the intrinsic r_0.

Registry No. $C_{16}PN$, 93597-88-7; PLA_2, 9001-84-7; $proPLA_2$, 37350-21-3; Trp, 73-22-3.

REFERENCES

Allegrini, P. R., van Scharrenburg, G. J. M., Slotboom, A. J., de Haas, G. H., & Seelig, J. (1985) *Biochemistry 24*, 3268.

Bevington, P. V. (1969) *Data Reduction and Error Analysis for the Physical Sciences*, McGraw-Hill, New York.

Cross, A. J., & Fleming, G. R. (1984) *Biophys. J. 46*, 45.

Dijkstra, B. W., Kalk, K. H., Drenth, J., & Vandermaelen, P. J. (1978) *J. Mol. Biol. 124*, 53.

Dijkstra, B. W., Kalk, K. H., Hol, W. G. J., & Drenth, J. (1981a) *J. Mol. Biol. 147*, 9.

Dijkstra, B. W., Drenth, J., & Kalk, K. H. (1981b) *Nature (London) 289*, 604.

Dijkstra, B. W., van Nes, G. J. H., Kalk, K. H., Brandenburg, N. P., Hol, W. G. J., & Drenth, J. (1982) *Acta Crystallogr., Sect. B: Struct. Crystallogr. Cryst. Chem. B38*, 793.

Dijkstra, B. W., Renetseder, R., Kalk, K. H., Hol, W. G. J., & Drenth, J. (1983) *J. Mol. Biol. 168*, 163.

Donne-Op den Kelder, G. M., Hille, J. D. R., Dijkman, R., de Haas, G. H., & Egmond, M. R. (1981) *Biochemistry 20*, 4074.

Eftink, M. (1983) *Biophys. J. 43*, 323.

Fletcher, R., & Powell, M. J. D. (1963) *Comput. J. 6*, 163.

Grinvald, A., & Steinberg, I. Z. (1974) *Anal. Biochem. 54*, 583.

Hille, J. D. R., Donne-Op den Kelder, G. M., Sauve, P., de Haas, G. H., & Egmond, M. R. (1981) *Biochemistry 20*, 4068.

Himmelblau, D. M. (1972) *Applied Nonlinear Programming*, McGraw-Hill, New York.

Huber, R., & Bode, W. (1978) *Acc. Chem. Res. 11*, 114.

Huber, R., & Bennett, W. S. (1983) *Biopolymers 22*, 261.
Hudson, B., & Cavalier, S. A. (1988) in *Spectroscopic Membrane Probes* (Loew, L., Ed.) CRC, Boca Raton, FL.
Hudson, B., Harris, D. L., Ludescher, R. D., Ruggiero, A., Cooney-Freed, A., & Cavalier, S. A. (1986) in *Fluorescence in the Biological Sciences* (Taylor, D. L., Waggoner, A. S., Lanni, F., Murphy, R. F. & Birge, R., Eds.) pp 159-202, Alan R. Liss, New York.
Hudson, B., Ludescher, R. D., Ruggiero, A., Harris, D. L., & Johnson, I. (1987) *Comm. Mol. Cell. Biophys. 4*, 171.
Jansen, E. H. J. M. (1979) Ph.D. Dissertation, State University of Utrecht, The Netherlands.
Jones, T. A. (1978) *J. Appl. Crystallogr. 11*, 268.
Kasprzak, A., & Weber, G. (1982) *Biochemistry 21*, 5924.
Kinosita, K., Kawato, S., & Ikegami, A. (1977) *Biophys. J. 20*, 289.
Lakowicz, J. R., Maliwal, B. P., Cherek, H., & Balter, A. (1983) *Biochemistry 22*, 1741.
Lindblom, G., & Wennerstrom, H. (1979) *Biophys. Chem. 6*, 167.
Lipari, G., & Szabo, A. (1980) *Biophys. J. 30*, 489.
Ludescher, R. D. (1984a) *Biophys. J. 45*, 336a.
Ludescher, R. D. (1984b) Ph.D. Dissertation, University of Oregon, Eugene, OR.
Ludescher, R. D., Volwerk, J. J., de Haas, G. H., & Hudson, B. S. (1985) *Biochemistry 24*, 7240.
Ludescher, R. D., Peting, L., Hudson, S., & Hudson, B. (1987) *Biophys. Chem. 28*, 59.
Marquardt, D. W. (1963) *J. Soc. Ind. Appl. Math. 11*, 431.
Nieuwenhuizen, W., Kunze, H.,, & de Haas, G. H. (1974) *Methods. Enzymol. 32B*, 147.
Papenhuijzen, J., & Visser, A. J. W. G. (1983) *Biophys. Chem. 17*, 57.
Ruggiero, A. J., & Hudson, B. (1988) *Biophys. J.* (in press).
Sklar, L. A., Hudson, B. S., & Simoni, R. D. (1977) *Biochemistry 16*, 819.
Slotboom, A. J., Jansen, E. H. J. M., Pattus, F., & de Haas, G. H. (1978) in *Semisynthetic Peptides and Proteins* (Offord, R. E., & DiBello, C., Eds.) pp 315-348, Academic, London.
Small, E. W., Libertini, L., & Isenberg, I. (1984) *Rev. Sci. Instrum. 55*, 879.
Soares de Araujo, P., Rosseneu, M. Y., Kremer, J. M. H., van Zoelen, E. J. J., & de Haas, G. H. (1979) *Biochemistry 18*, 580.
Valeur, B., & Weber, G. (1977) *Photochem. Photobiol. 25*, 441.
Van Dam-Mieras, M. C. E., Slotboom, A. J., Pieterson, W. A., & de Haas, G. H. (1975) *Biochemistry 14*, 5387.
Volwerk, J. J., & de Haas, G. H. (1982) in *Lipid-Protein Interactions* (Jost, P., & Griffith, O. H., Eds.) Vol. 1, pp 69-149, Wiley, New York.
Volwerk, J. J., Jost, P. C., de Haas, G. H., & Griffith, O. H. (1985) *Chem. Phys. Lipids 36*, 101.
Weber, G. (1960) *Biochem. J. 75*, 345.
Wennerstrom, H., & Lindman, B. (1979) *Phys. Rep. 52*, 1.
Yamamoto, Y., & Tanaka, J. (1972) *Bull. Chem. Soc. Jpn. 45*, 1362.

Mechanism of Azide Binding to Chloroperoxidase and Horseradish Peroxidase: Use of an Iodine Laser Temperature-Jump Apparatus†

Josef F. Holzwarth,‡ Frank Meyer,‡ Michael Pickard,§ and H. Brian Dunford*,‖
Fritz-Haber-Institut der Max-Planck-Gesellschaft, Faradayweg 4-6, D-1000 Berlin 33, West Germany, and Departments of Microbiology and Chemistry, University of Alberta, Edmonton, Alberta, Canada T6G 2G2
Received February 12, 1988; Revised Manuscript Received April 22, 1988

ABSTRACT: The kinetics of azide binding to chloroperoxidase have been studied at eight pH values ranging from 3.0 to 6.6 at 9.5 ± 0.2 °C and ionic strength of 0.4 M in H_2O. The same reaction was studied in D_2O at pD 4.36. In addition, results were obtained on azide binding to horseradish peroxidase at pD 4.36 and pH 4.56. Typical relaxation times were in the range 10–40 μs. The value of k_H/k_D(on) for chloroperoxidase is 1.16, and k_H/k_D(off) is 1.7; corresponding values for horseradish peroxidase are 1.10 and 2.4. The H/D solvent isotope effects indicate proton transfer is partially rate controlling and is more important in the dissociation of azide from the enzyme–ligand complex. A mechanism is proposed in which hydrazoic acid binds to chloroperoxidase in a concerted process in which its proton is transferred to a distal basic group. Hydrogen bonding from the newly formed distal acid to the bound azide facilitates formation of hydrazoic acid as the leaving group in the dissociation process. The binding rate constant data, k_{on}, can be fit to the equation $k_{on} = k_3/(1 + K_A/[H^+])$, where $k_3 = 7.6 \times 10^7$ M^{-1} s^{-1} and K_A, the dissociation constant of hydrazoic acid, is 2.5×10^{-5} M. The same mechanism probably is valid for the ligand binding to horseradish peroxidase.

Azide is a well-known inhibitor of many enzyme systems. The study of the kinetics of azide binding to heme enzymes has been hampered because the relaxation time of the reaction falls within the dead time of most instrumental techniques. Thus, the kinetics of azide binding to horseradish peroxidase required the use of an ultrafast (coaxial cable) temperature-jump apparatus (Morishima et al., 1978). In this paper we report on the kinetics of azide binding to chloroperoxidase at eight pH values over the accessible pH range using an ILTJ[1]

† Supported by the Deutsche Forschungsgemeinschaft and the Natural Sciences and Engineering Research Council of Canada.
* Author to whom correspondence should be addressed.
‡ Fritz-Haber-Institut der Max-Planck-Gesellschaft.
§ Department of Microbiology, University of Alberta.
‖ Department of Chemistry, University of Alberta.

[1] Abbreviations: ILTJ, iodine laser temperature-jump apparatus; R.Z., reinheitzahl (purity number).

0006-2960/88/0427-6628$01.50/0